SAE TECHNICAL PAPER SERIES

2007-01-2682

E

A Nonlinear Kalman Filter Algorithm for Monitoring the Motion of a Vehicle in Real Time Around a Reference Trajectory

Jairo Cavalcanti Amaral
Instituto Nacional de Pesquisas Espaciais-INPE

Marcelo Lopes de Oliveira e Souza
Insituto Nacional de Pesquisas Espaciais-INPE

SAE BRASIL
Sociedade de Engenheiros da Mobilidade

FILIADA À
SAE International

Congresso 2007
SAE BRASIL

XVI Congresso e Exposição Internacionais da Tecnologia da Mobilidade
São Paulo, Brasil
28 a 30 de novembro de 2007

AV. PAULISTA, 2073 - HORSA II - CJ. 1003 - CEP 01311-940 - SÃO PAULO – SP

2007-01-2682

A Non linear Kalman Filter Algorithm for Monitoring the Motion of a Vehicle in Real Time Around a Reference Trajectory

Jairo Cavalcanti Amaral
Marcelo Lopes de Oliveira e Souza
Hélio Koiti Kuga
Instituto Nacional de Pesquisas Espaciais-INPE

ABSTRACT

In this work, we present a nonlinear Kalman filter algorithm for monitoring the orbital motion of a single satellite in real time, changing the used observing sources according to convenience. The errors in orbit determination will ultimately affect the performance of the control and maneuvering of the satellite, providing the basis for future corrective and preventive satellite maintenance.

INTRODUCTION

The problem to be solved here is to develop a nonlinear Kalman filter algorithm which uses real-time measurements to produce estimates of a satellite position and velocity – the best possible for the information available. The algorithm will allow a preliminary study of the filter behavior in face of varying parameters such as measurement precision and measurement rate. This can later be extended to provide good preventive/corrective maintenance of a satellite constellation, where it is necessary to have precise estimations of the satellite positions to support maintenance decisions.

SYSTEM DESCRIPTION

The simulated satellite has an orbit in a bidimensional space, and the measurements considered are three simultaneous distances from it taken by other four satellites simulated at GPS-altitude orbits in the same plane.

The state vector **x** contains the position (x_1, x_2) and velocity (x_3, x_4) of the simulated satellite in each dimension (x, y), while the vector of observation **y** contains the distances from the simulated satellite observed by the other three GPS satellites. Below, **G** is the dynamic noise addition matrix, **ω** is the **continuous** dynamic noise vector, assumed normal with zero mean and covariance **Q**; and **v** is the **discrete** observation noise vector, assumed normal with zero mean and covariance **R**. The Earth gravitational parameter considered in the simulations is μ = 398600 km^3/s^2. So, the equations of the system are:

$$\begin{cases} \dot{\mathbf{x}}(t) = \mathbf{f}(\mathbf{x}(t)) + \mathbf{G}\boldsymbol{\omega}(t), \forall t \in [t_0; t_f] \\ \mathbf{y}(t_i) = \mathbf{h}(\mathbf{x}(t_i)) + \mathbf{v}(t_i), t_i = t_0 + i.T_s, i = 1,2,3...N_s \end{cases} \quad (1)$$

where $\boldsymbol{\omega} = N(\mathbf{0}, \mathbf{Q})$ and $\mathbf{v} = N(\mathbf{0}, \mathbf{R})$.

The functions of transition **f**(**x**) and observation **h**(**x**) are described as follows:

$$\mathbf{f}(\mathbf{x}) = \begin{bmatrix} x_3 \\ x_4 \\ -\frac{\mu}{r^3} x_1 \\ -\frac{\mu}{r^3} x_2 \end{bmatrix} \quad (2)$$

where $r = \sqrt{x_1^2 + x_2^2}$ is the orbit radius magnitude.

$$\mathbf{h}(\mathbf{x}) = \begin{bmatrix} \sqrt{(x_1 - X_1)^2 + (x_2 - Y_1)^2} \\ \sqrt{(x_1 - X_2)^2 + (x_2 - Y_2)^2} \\ \sqrt{(x_1 - X_3)^2 + (x_2 - Y_3)^2} \end{bmatrix} \quad (3)$$

where X_i, Y_i, are the position coordinates of the observing GPS satellite i.

FILTER DESCRIPTION

The Kalman filter [1] works by trying to minimize the mean squared estimation error of the state of linear systems with noises in the dynamics and in the measurements. According to references such as [2-4], it has the advantage that it can be used recursively, instead of being obliged to collect and process all data at once as other minimum

square methods. Besides that, it can easily include the dynamic noise in the formulation. It consists of two phases: 1) propagation in time, where it takes initial estimates of the mean state vector $\bar{\mathbf{x}}(t)$ and the state covariance matrix $\mathbf{P}(t)$ and predicts their behavior until the next measurements; and 2) updating in measure, where it uses the available measurements to obtain new estimates by comparing them with propagated ones.

The mean state vector $\bar{\mathbf{x}}(t)$ will follow the (ideal) physical model without noise, but the uncertainty (given by the covariance matrix $\mathbf{P}(t)$) will be updated taking into account the uncertainties attributed to the model. The Kalman filter theory assumes normal distributions of deviations; actually they are not always normal, but this is a fair approximation in most cases.

As most things in Nature, satellites in orbit do not exhibit linear behavior, so we need to use linear approximations in a variant called **the extended Kalman filter**. At the initial instant t_0, it starts the first nominal state trajectory $\mathbf{x}_n(t)$ in the initial state estimate $\mathbf{x}_0$, i.e., $\mathbf{x}_n(t_0) = \bar{\mathbf{x}}(t_0) = \mathbf{x}_0$. Between updating instants (t_i; t_{i+1}) it propagates the nominal state trajectory $\mathbf{x}_n(t)$, as being the mean trajectory $\bar{\mathbf{x}}(t)$, i.e., $\mathbf{x}_n(t) = \bar{\mathbf{x}}(t)$ from that point on, until the new updating. At each updating instant t_i, it starts a new $\mathbf{x}_n(t)$ in the updated state estimate $\hat{\mathbf{x}}(t_i)$, i.e., $\mathbf{x}_n(t_i) = \hat{\mathbf{x}}(t_i)$. While more computationally costly, it is more adequate to situations of poor models or initial conditions and it is easier to implement than its counterpart called **the linearized Kalman filter**, which works only with the linear deviations from a nominal trajectory $\mathbf{x}_n(t)$ that is not altered along the cycles. In this paper, we will use the extended Kalman filter.

PROPAGATION PHASE – **Considering a continuous system and a discrete measurement**, the propagation phase of $\bar{\mathbf{x}}(t)$ and $\mathbf{P}(t)$ during $t \in (t_i; t_{i+1})$ is defined by the following differential equation system:

$$\begin{cases} \dot{\bar{\mathbf{x}}} = \mathbf{f}(\bar{\mathbf{x}}), \bar{\mathbf{x}}(t_0) = \mathbf{x}_0 \\ \dot{\bar{\mathbf{P}}} = \mathbf{F}\bar{\mathbf{P}} + \bar{\mathbf{P}}\mathbf{F}^T + \mathbf{G}\mathbf{Q}\mathbf{G}^T, \bar{\mathbf{P}}(t_0) = \mathbf{P}_0 \end{cases} \quad (4)$$

where $\mathbf{F}$ is the jacobian matrix of $\mathbf{f}$:

$$\mathbf{F} = \left.\frac{\partial \mathbf{f}}{\partial \mathbf{x}}\right|_{\mathbf{x}=\mathbf{x}_n(t)} = \begin{bmatrix} 0 & 0 & 1 & 0 \\ 0 & 0 & 0 & 1 \\ 3\mu r^{-5}x_1^2 - \mu r^{-3} & 3\mu r^{-5}x_1 x_2 & 0 & 0 \\ 3\mu r^{-5}x_2 x_1 & 3\mu r^{-5}x_2^2 - \mu r^{-3} & 0 & 0 \end{bmatrix} \quad (5)$$

with $r = \sqrt{x_1^2 + x_2^2}$.

UPDATING PHASE – The updating phase at $t = t_i$ is done by first defining the Kalman gain $\mathbf{K}$, and then using it to find the updated $\bar{\mathbf{x}}(t)$ and $\mathbf{P}(t)$:

$$\mathbf{K} = \bar{\mathbf{P}}\mathbf{H}^T\left(\mathbf{H}\bar{\mathbf{P}}\mathbf{H}^T + \mathbf{R}\right)^{-1} \quad (6)$$

$$\hat{\mathbf{P}} = (\mathbf{I} - \mathbf{K}\mathbf{H})\bar{\mathbf{P}} \quad (7)$$

$$\hat{\mathbf{x}} = \bar{\mathbf{x}} + \mathbf{K}\left[\mathbf{y} - \mathbf{h}(\bar{\mathbf{x}})\right] \quad (8)$$

with

$$\mathbf{H} = \left.\frac{\partial \mathbf{h}}{\partial \mathbf{x}}\right|_{x=x_n(t_k)} = \begin{bmatrix} \frac{(x_{n1} - X_1)}{C_1} & \frac{(x_{n2} - Y_1)}{C_1} & 0 & 0 \\ \frac{(x_{n1} - X_2)}{C_2} & \frac{(x_{n2} - Y_2)}{C_2} & 0 & 0 \\ \frac{(x_{n1} - X_3)}{C_3} & \frac{(x_{n2} - Y_3)}{C_3} & 0 & 0 \end{bmatrix} \quad (9)$$

where

$$\begin{cases} C_1 = \sqrt{(x_{n1} - X_1)^2 + (x_{n2} - Y_1)^2} \\ C_2 = \sqrt{(x_{n1} - X_2)^2 + (x_{n2} - Y_2)^2} \\ C_3 = \sqrt{(x_{n1} - X_3)^2 + (x_{n2} - Y_3)^2} \end{cases} \quad (10)$$

The new $\hat{\mathbf{x}}$ and $\hat{\mathbf{P}}$ are then used for initializing the next propagation phase.

DESCRIPTION OF THE SIMULATED CASES

The positions of each satellite were produced by a numerical simulation with MatLab (versions 6.1) using the two body dynamics, as described in [5]. For the observed satellite, a dynamic noise was introduced as an acceleration in each dimension to account for the imprecision of the model. Eclipses in observation caused by Earth were neglected. In the simulations using the data from all four observing satellites, the algorithm always uses the three closest, reassigning the farthest to the next to farthest slot at the instant they change places.

The simulation parameters (absolute tol. = 10^{-6}, relative tol. = 10^{-8}) were chosen so that, with dynamic noise $\sigma_D = 0$, the order of the numerical error in position after one revolution be smaller than 1 m, using the variable step integration methods ODE1-13 of Matlab 6.1. We plotted the results for each satellite in N equally distributed instants along the time span $[t_0;t_f]$. In the same time interval the measurements were done at a rate T_s. The observed satellite

initial conditions $\mathbf{x}_0 = \mathbf{x}(t_0)$ are assumed to be known with a standard deviation σ_P at each dimension of position and σ_V at each dimension of velocity; the dynamic noise has a standard deviation σ_D in each dimension, and the measurement noise has a standard deviation σ_M in each sensor.

The tests were conducted according to Table 1, by applying deviations in the initial conditions $\mathbf{x}_0 = \mathbf{x}(t_0)$ that were equal to the uncertainty attributed to them, and then letting the Kalman filter try to approach the actual positions by using the measurements affected by noise.

Table 1: Parameters of the Graphics Shown in Figures 1-14.

Tests	σ_M	σ_D	T_s	Initial State $x(t_0)$	Initial Estimate $\bar{\mathbf{x}}_0$	Initial Covariance P_0 (diagonal)
Figure 1	10 m	1e-3 m/s2	60 s	[7000, 0, 0, 7.5]	[7010, 10, 1, 8.5]	[10^2, 10^2, 1^2, 1^2]
Figure 2	10 m	1e-3 m/s2	60 s	[7000, 0, 0, 7.5]	[7010, 10, 1, 8.5]	[10^2, 10^2, 1^2, 1^2]
Figure 3	10 m	1e-3 m/s2	60 s	[7000, 0, 0, 7.5]	[7010, 10, 1, 8.5]	[10^2, 10^2, 1^2, 1^2]
Figure 4	1km	1e-3 m/s2	60 s	[7000, 0, 0, 7.5]	[7010, 10, 1, 8.5]	[10^2, 10^2, 1^2, 1^2]
Figure 5	6 m	1e-3 m/s2	60 s	[7000, 0, 0, 7.5]	[7010, 10, 1, 8.5]	[10^2, 10^2, 1^2, 1^2]
Figure 6	10 m	1e-3 m/s2	120 s	[7000, 0, 0, 7.5]	[7010, 10, 1, 8.5]	[10^2, 10^2, 1^2, 1^2]
Figure 7	10 m	1e-3 m/s2	10 s	[7000, 0, 0, 7.5]	[7010, 10, 1, 8.5]	[10^2, 10^2, 1^2, 1^2]
Figure 8	10 m	1e-2 m/s2	10 s	[7000, 0, 0, 7.5]	[7010, 10, 1, 8.5]	[10^2, 10^2, 1^2, 1^2]
Figure a9	100 m	1e-3 m/s2	60 s	[7000, 0, 0, 7.5]	[7010, 10, 1, 8.5]	[10^2, 10^2, 1^2, 1^2]
Figure 10	100 m	1e-3 m/s2	60 s	[7000, 0, 0, 7.5]	[7010, 10, 1, 8.5]	[10^2, 10^2, 1^2, 1^2]
Figure 11	100 m	1e-3 m/s2	60 s	[7000, 0, 0, 7.5]	[7010, 10, 1, 8.5]	[10^2, 10^2, 1^2, 1^2]
Figure 12	100 m	1e-3 m/s2	60 s	[7000, 0, 0, 7.5]	[7010, 10, 1, 8.5]	[10^2, 10^2, 1^2, 1^2]
Figure 13	10 m	1e-3 m/s2	60 s	[7000, 0, 0, 7.5]	[7010, 10, 1, 8.5]	[10^2, 10^2, 1^2, 1^2]
Figure 14	10 m	1e-3 m/s2	60 s	[7000, 0, 0, 7.5]	[7010, 10, 1, 8.5]	[10^2, 10^2, 1^2, 1^2]

Though the estimation process does not require this, we also recovered the positions pointed by the noisy measurements for comparison with the real and estimated positions. The method chosen was a Newton-Raphson iteration using the first two of the three distances measured. As the observed satellite is assumed to be always in a lower orbit than the GPS', the initial radius is equaled to zero and then used in the following recursion:

$$\mathbf{r}_{k+1} = \mathbf{r}_k + \left[\frac{\partial \mathbf{h}(\mathbf{r}_k)}{\partial \mathbf{r}}\right]^{-1} \left[\boldsymbol{\rho} - \mathbf{h}(\mathbf{r}_k)\right] \qquad (11)$$

until $\left\|\mathbf{r}_{k+1} - \mathbf{r}_k\right\| \le \varepsilon$, where $\varepsilon = 0.0001$ is the desired precision.

In a real time application, the algorithm would start propagating the initial state vector and covariance matrix and stop at the scheduled time of the next measure until it comes; then repeat the procedure with the updated state.

RESULTS

Figure 1 and 3 show that the Kalman filter was able to estimate the position and velocity beyond the measurement error, even with measures related only to position. The algorithm was able to drop the position standard deviation from 10 km to 5 meters in 10 to 20 measurements of 10 m precision, and the velocity standard deviation from 1 km/s to less than 10 cm/s in an equivalent time interval.

With the standard parameters of the first example, position and velocity deviations ultimately settled around 5 m and 3 cm/s respectively. Besides that:

Figures 1 and 2 show that the standard deviation of *x* and *y* axis are oscillating and opposed to each other.

Figures 1 and 4 show that decreasing the measurement precision by two orders caused a decrease in estimate precision in more than 10 times, and a longer transient.

Figures 1 and 5 show that increasing the measurement precision to 6 m caused the estimation precision to increase to 4 m or better.

Figures 1 and 6 show that increasing the sampling period by 2 reduced the estimating precision to around 7 m.

Figures 1 and 7 show that reducing the sampling period to 10 seconds increased the estimating precision to around 3 m.

Figures 1 and 8 show that increasing the dynamic noise in one order caused the estimating precision to decrease to around 10 m.

Figure 9 shows the deviation and uncertainty in the *x* axis position, when only 3 fixed sources are used. Figure 10 shows the same, but using alternated data from 4 satellites. The instants of change are most easily perceived as irregularities in the sinusoidal pattern of the standard deviation envelope.

Figure 11 shows the three measure slots against time when only 3 fixed sources are used. Figure 12 shows the same slots with the break points generated when they are reassigned to a better source.

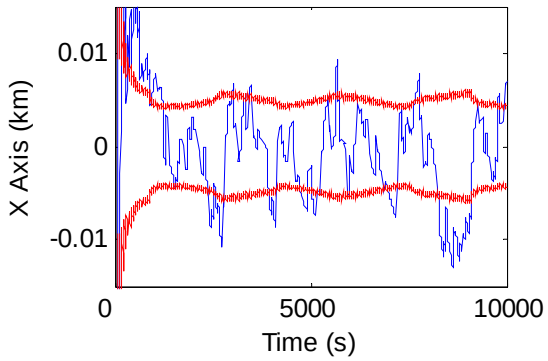

Fig. 1.

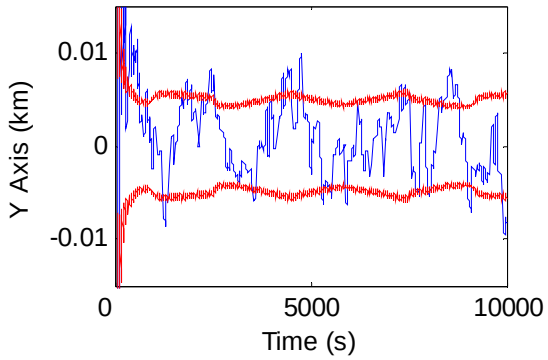

Fig. 2.

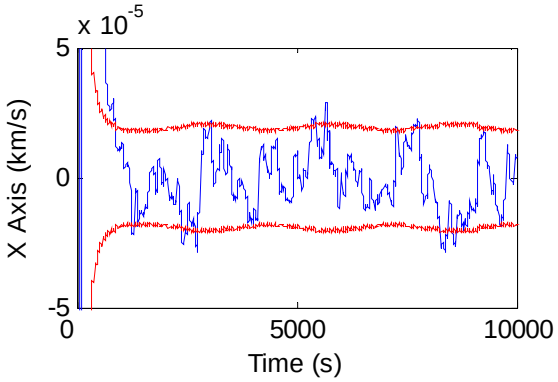

Fig. 3.

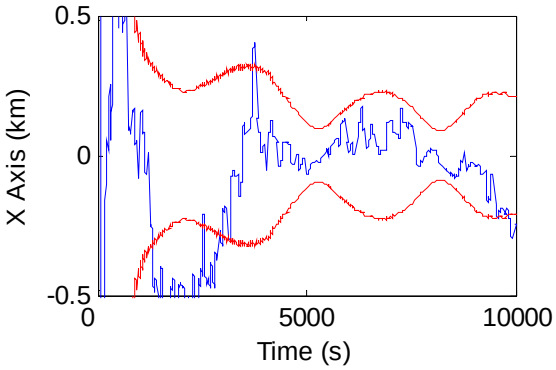

Fig. 4.

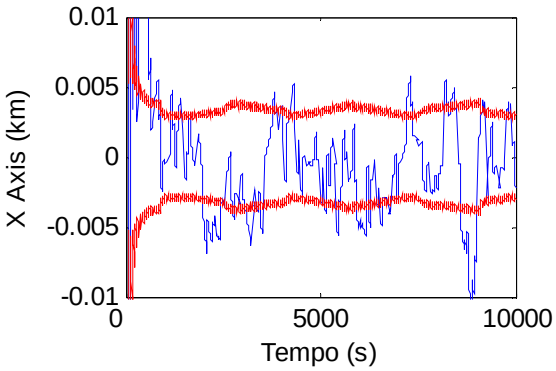

Fig. 5.

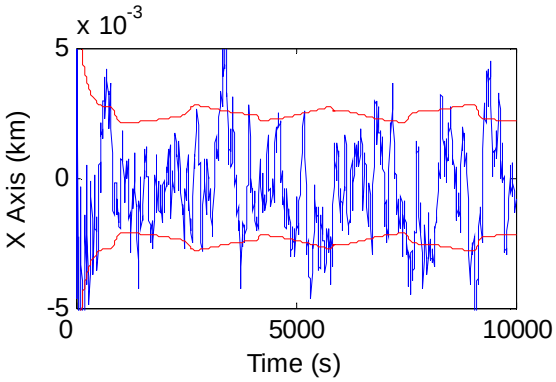

Fig. 7.

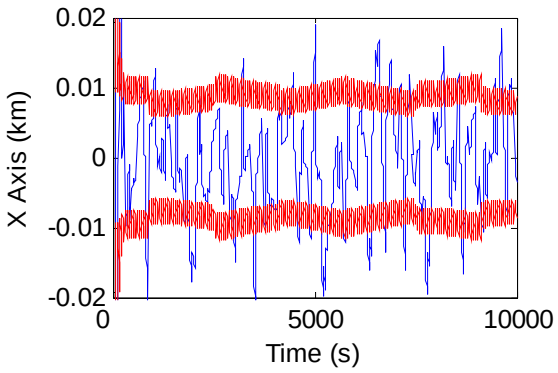

Fig. 8.

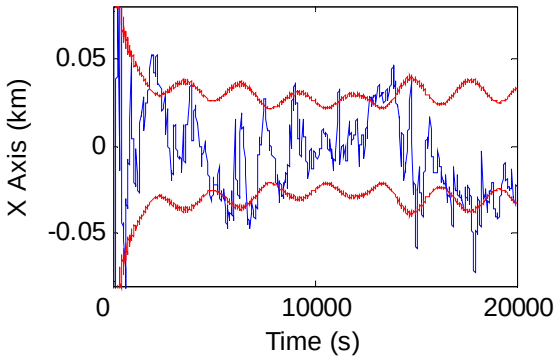

Fig. 9.

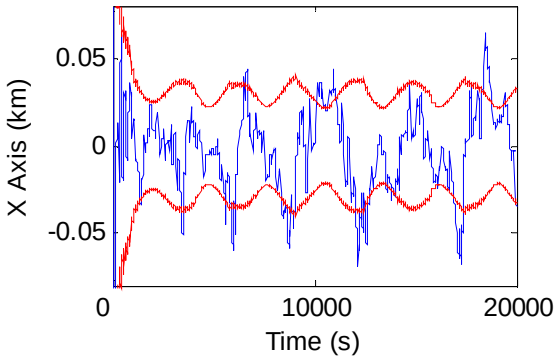

Fig. 10.

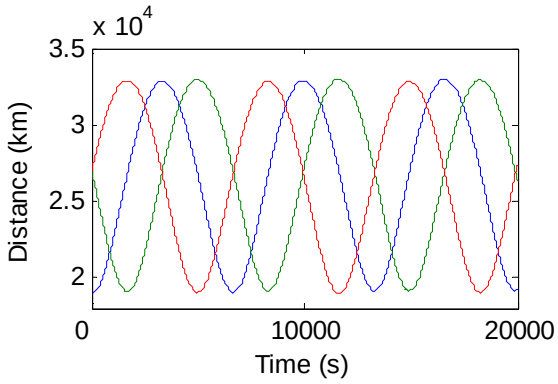

Fig. 11.

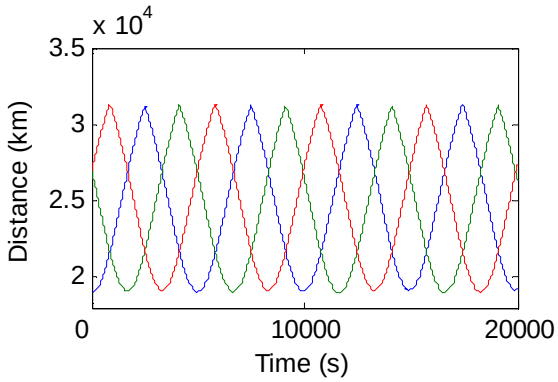

Fig. 12.

For didactic purposes, we also tested two less adequate variations in the algorithm, all of them with the same parameters shown in Fig 1.

Figure 13 shows the extended Kalman filter applied to a 3D space, i.e., **x** now includes z and v_z; but still with only 3 observers. As in tests 1-6 the three observing satellites were in the same plane of the observed satellite, and could only measure scalar distances, they had no means to observe the signal of the displacement in the z axis neither its speed. So, the linearization prevented any variation in z axis from being computed, since the first order derivatives $\frac{\partial \mathbf{h}}{\partial z}, \frac{\partial \mathbf{h}}{\partial v_z}$ are null at x-y plane. So, even with initial states zeroed in the z axis, the filter always diverged in a matter of time.

In Fig. 14, it was used the linearized Kalman filter, with an initial state of the nominal trajectory $\bar{\mathbf{x}}(t_0)$ deviated in 1 km along the x axis from the initial state of the real trajectory $\mathbf{x}(t_0)$. Differently from the extended Kalman filter, the nominal trajectory was not updated. It was able to work properly for one orbit; but, after that, the difference of position between the real and nominal references became too big, making the filter to diverge. As the standard deviation relies on the nominal trajectory, it did not accuse the divergence, which is even worse. This outweighs the milder computational load of this filter, and shows that it would be better only in situations where there is control to keep it close to the nominal trajectory.

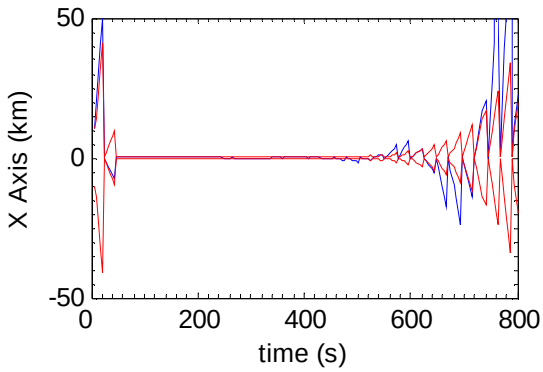

Fig. 13.

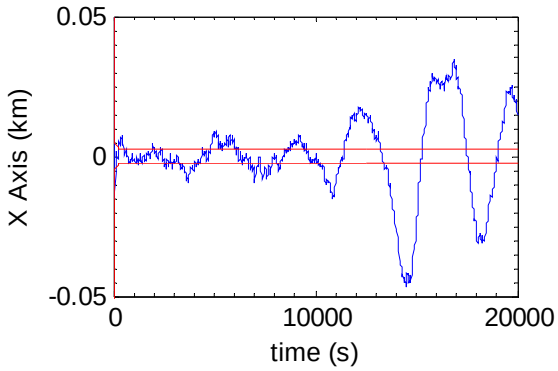

Fig. 14.

INTENDED EXTENTIONS

Until now the movements and deviations were kept in two dimensions. We intend to increase the number of observation sources used, so that we can also work in the *z* axis.

With the algorithm for a single satellite completed, the next step is to adapt it to a constellation of satellites and eventually include the modeling and detection of other GPS error sources, such as the clock synch and atmospheric interference, as treated in [6].

CONCLUSIONS

In this work, we presented a nonlinear Kalman filter algorithm for monitoring the orbital motion of a single satellite in real time. It was based on the extended Kalman filter mainly. Some tests were done to show its correctness. The tests helped to show how variations in the estimation parameters influence the quality of the resulting data. This is useful in determining what is necessary and what is superfluous, and is the key to find what parameters should be emphasized in a multi-satellite estimation system. After that, we intend to extend such algorithm to a triangular equatorial constellation of satellites to monitor their absolute positions and velocities.

ACKNOWLEDGMENTS

The first author thanks the National Council for Scientific and Technological Development-CNPq of Brazil for supporting him during this research. The second and third authors thank the National Institute for Space Research-INPE/DMC of Brazil for supporting them and the Laboratory of Computational Environments for Simulation, Identification, and Modeling LABSIM2 of AOCS where this work is being done.

REFERENCES

[1] Kalman, R.E., 1960, “A New Approach to Linear Filtering and Prediction Problems”, Transactions of the ASME–Journal of Basic Engineering, 82 (Series D): 35-45.

[2] Kuga, H.K., 2005, “Noções Práticas de Técnicas de Estimação”, INPE, São José dos Campos.

[3] Mybeck, P. S., 1979, “Stochastic Models, Estimation and Control”, vol.1, Academic Press, New York.

[4] Brown, R. G. and Hwang, P. Y. C., 1996, “Introduction to Random Signals and Applied Kalman Filtering”, John Wiley & Sons, New York.

[5] Kuga, H.K., Kondapali, R.R., 1995, “Introdução à Mecânica Orbital”, INPE-5615-PUD/064, INPE, São José dos Campos.

[6] Raimundo, P.C.P., 2007, “Determinação de Órbita via GPS Considerando Modelo de Pressão de Radiação Solar para o Satélite Topex/Poseidon”, INPE, São José dos Campos, Dissertação de Mestrado.

All SAE papers, standards, and selected books are abstracted and indexed in the Global Mobility Database.

ISSN 0148-7191